Assess the Intramolecular Cavity of a PAMAM Dendrimer in Aqueous Solution by Small-Angle Neutron Scattering

Tianfu Li,[†,‡] Kunlun Hong,[§] Lionel Porcar,[†,∥,⊥] Rafael Verduzco,[§] Paul D. Butler,[†] Gregory S. Smith,[#] Yun Liu,*[,†,⊥] and Wei-Ren Chen*[,#]

The NIST Center for Neutron Research, National Institute of Standards and Technology, Gaithersburg, Maryland 20899-8562; China Institute of Atomic Energy, P.O. Box 275-30, 102413, P. R. China; The Center for Nanophase Materials Sciences, Oak Ridge National Laboratory, Oak Ridge, Tennessee 37831; Institut Laue-Langevin, B.P. 156, F-38042 Grenoble Cedex 9, France; Department of Materials Science and Engineering, University of Maryland, College Park, Maryland 20742-2115; and Neutron Scattering Science Division, Spallation Neutron Source, Oak Ridge National Laboratory, Oak Ridge, Tennessee 37831

Received July 10, 2008; Revised Manuscript Received September 15, 2008

ABSTRACT: We present a contrast variation small-angle neutron scattering (SANS) study of a series of neutral PAMAM dendrimers in aqueous solutions using three different generations (G4−6) at a concentration of about 10 mg/mL. Varying the solvent hydrogen−deuterium ratio, the scattering contributions from the water molecules and the constituent components of PAMAM dendrimer can be determined. Using an analytical model of the scattering cross section $I(Q)$ incorporating the effect of water penetration, we have quantified the intramolecular space of PAMAM dendrimer by evaluating the number of guest water molecules, and we draw a direct comparison to computational predictions. As expected, the overall available internal cavity was seen to increase as a function of increasing dendrimer generation. However, the fraction of water accessible volume of a dendrimer was found to remain invariant for the three generation PAMAM dendrimers studied in this report. We have also estimated the average water density inside a dendrimer, which is found to be higher than that of bulk water.

I. Introduction

Dendrimers are man-made macromolecules with a highly regular three-dimensional architecture. They are synthesized stepwise by a repetitive procedure, which starts from the multifunctional core molecule and covalently links new branched units of monomers to the peripheral end groups to form a higher generation.[1] Dendrimers have been extensively explored as possible drug and gene delivery agents.[2] These applications arise not only from their unique combination of intrinsic properties such as the presence of interior cavities, monodisperse nanosized structure, and chemical uniformity but also from their water solubility, nonimmunogenicity, and biocompatibility via tailoring the functionalizable architecture. Presently, more than 100 families of dendrimers with more than 1000 kinds of multifunctional surface groups have been synthesized. However, polyamidoamine starburst dendrimers (PAMAM) with ethylenediamine (EDA) cores are one of the most studied types of dendrimers due to the simple method of synthesis and vast potential applications.[3]

To be able to be processed as an emerging delivery system, thorough characterization of the structural properties of the dendrimers is required to optimize and develop their specific applications. One of the major focuses for computational studies is to evaluate the dendrimer intramolecular space available for accommodating any guest molecules. The internal accessible volume of generation 4 to 8 (G4−8) PAMAM dendrimers in various solvent conditions have been first calculated with computer simulations by Goddard et al.[4−6] The size of the internal voids is quantitatively estimated by calculating the total space occupied by water molecules penetrating the dendrimer architecture. As expected, the average number of water molecules associated with a single dendrimer is found to increase steadily upon increasing the dendrimer generation, indicating a gradual increase in the overall solvent accessible internal volume. Later, a similar conclusion has also been reached by Wagner et al.[7] and Larson et al.[8] in their recent molecular dynamics simulations carried out by taking into account explicitly water molecules.

The purpose of this work is to provide the comparative experimental evidence to gauge the accuracy of these computational predictions. An experimental approach, combining the small-angle neutron scattering (SANS) technique and contrast variation method, is used to evaluate the PAMAM dendrimer internal space accessible to water molecules as a function of the generation.

It is not novel to use the SANS technique, combined with contrast variation method, to examine the structural properties of dendrimer solutions: A series of systematic experimental investigations have focused on understanding the intramolecular density profile: On the basis of the dendrimer spatial distribution of the isotope-labeled terminal groups, Ballauff et al. have concluded by SANS data analysis that the intramolecular density exhibits its maximum at the center of the molecule and decreases toward the periphery.[9,10] However, an intrinsically different picture, namely the dense-shell profile, is obtained by Amis et al. based on the conclusion of SANS experiments with essentially the same molecular design.[11] Moreover, the contrast variation SANS method has been used by Durbin et al.[12] and Imae et al.[13] to explore the counterion distribution around charged carboxyl-terminated dendrimers and the evolution of radius of gyration R_G of the dendrimer with hydroxyl end groups as a function of the isotopic ratio of the solvent.

Different from the previously reported experiments, our SANS study using the contrast variation method focuses on providing structural information about the internal space of a

* Corresponding authors. E-mail: yunliu@nist.gov; chenw@ornl.gov.
† National Institute of Standards and Technology.
‡ China Institute of Atomic Energy.
§ The Center for Nanophase Materials Sciences, Oak Ridge National Laboratory.
∥ Institut Laue-Langevin.
⊥ University of Maryland.
Spallation Neutron Source, Oak Ridge National Laboratory.

10.1021/ma801555j CCC: $40.75
Published on Web 10/25/2008

dendrimer molecule via the estimation of the average number of associated water molecules. The contrast of a dendrimer in respect to the solvent is adjusted by tuning the molecular ratio of H_2O and D_2O. A theoretical model for the SANS differential cross section incorporating the H/D exchange fraction is developed to analyze the SANS absolute intensity distributions. Our estimated number of water molecules in a dendrimer is in excellent quantitative agreement with the computer simulation result when an appropriate molecular boundary radius is chosen. We find that the fraction of the water accessible volume over the total volume of a dendrimer remains almost constant from generation 4 to 6. By assuming that the specific volume of a dendrimer does not change for the different solvent conditions, the average water density inside a dendrimer can be calculated, and its value is found to be higher than the one of bulk water.

II. Materials and Methods

Materials. Biomedical grade generation 4−6 PAMAM dendrimers were purchased from Dendritech Inc., Midland, MI.[14] Deuterium oxide (catalogue number DLM-6-10X1) was obtained from Cambridge Isotope Laboratories, Inc., Andover, MA.[14] The procedure of sample preparation is described elsewhere.[15] In this study, the dendrimer concentration of the samples used in the SANS experiment was kept at about 10 mg/mL, which is chosen as a compromise between minimizing the scattering contribution from inter-dendrimer correlation which could potentially complicate the data analysis and maintaining a satisfactory signal-to-noise ratio in the scattering patterns within a reasonable experimental time.

Small-Angle Neutron Scattering (SANS). SANS measurements were performed on the NG-3 SANS instrument at NIST Center for Neutron Research. The wavelength of the incident neutrons beam was set at 6.0 Å, with wavelength spread $\Delta\lambda/\lambda$, of 15%, and the corresponding wave vector Q was ranging from 0.02 to 0.45 $Å^{-1}$ with the selected sample-to-detector distances. The samples were contained in 1 mm path length quartz cells. The samples were used immediately after purification and all the experiments were carried out at room temperature. The measured intensity was also corrected for detector background and sensitivity and for scattering contributed from the empty cells and placed in an absolute scale using a direct beam measurement.[16]

Theoretical Basis. The SANS intensity distribution $I(Q)$ obtained from the PAMAM dendrimer in aqueous solutions is given by the following analytical expression

$$I(Q) = AP(Q)S(Q) + I_{INC} \tag{1}$$

where A is the scattering amplitude depending on the contrast, $P(Q)$ the normalized intramolecular structure factor, $S(Q)$ the interdendrimer structure factor, and I_{INC} the incoherent background. The contribution of the interdendrimer correlation to $I(Q)$ is found to be negligible in our diluted samples when the Coulomb interaction can be ignored. Therefore, $S(Q)$ can be well approximated as unity. Consequently, $I(Q)$ is dominated by $P(Q)$. A previous developed analytical model for $P(Q)$ is used to analyze the scattering patterns, and its detailed description is given elsewhere.[15] In this model, $P(Q)$ is given as follows:

$$P(Q) = \left\{\frac{3}{(QR_{HS})^3}[\sin(QR_{HS}) - QR_{HS}\cos(QR_{HS})]\exp\left(-\frac{Q^2\sigma^2}{4}\right)\right\}^2 + a_b P_{fluc}(Q, R_G) \tag{2}$$

In this expression, the first term gives the contribution of the whole shape, a homogeneous hard sphere with radius R_{HS} and fuzzy edge σ. The second term gives the contribution from the intradendrimer density fluctuations, which has been discussed in ref. 15. The radius of gyration R_G is expressed analytically as

$$R_G^2 = \frac{3}{10}(2R_{HS}^2 + 5\sigma^2) \tag{3}$$

Assuming the incompressible mixture of water and dendrimer, the amplitude factor A appearing in eq 1 is given explicitly in the following expression:

$$A = nN_A\left\{\sum b_{dendr} + \gamma N_{ex}(b_D - b_H) - \frac{\upsilon_{dendr}}{\upsilon_{water}}[b_{H_2O} + \gamma(b_{D_2O} - b_{H_2O})]\right\}^2 \tag{4}$$

where n is the molar concentration of the dendrimers, N_A is the Avogadro number, $\sum b_{dendr}$ is the total scattering length of all atoms in a dendrimer molecule, b_D, b_H, b_{H_2O}, and b_{D_2O} representing the scattering length of D, H, H_2O, and D_2O, respectively, υ_{dendr} is the volume of the constituent components of a single dendrimer, υ_{water} is the molecular volume of water (30 $Å^3$), γ is the molar fraction of D_2O, and N_{ex} is the total number of exchangeable proton in a single dendrimer molecule. It is known that the protons present in the primary and secondary amine groups are all labile to exchange.[17] Consequently, for a given dendrimer generation p, N_{ex} can be expressed as

$$N_{ex} = 2^{p+4} - 4 \tag{5}$$

The only unknown parameter υ_{dendr} in eq 4 can be calculated from the different amplitude factors obtained from samples with different γ values. The water accessible volume inside the dendrimer molecule can be calculated by subtracting υ_{dendr} from the overall molecular volume estimated from the structural parameters R_{HS} and σ obtained from the model fitting.

Equation 4 is only valid when the water density inside and outside the dendrimer remain identical. If the average water density inside a dendrimer changes by a factor of α compared to the bulk water value, the scattering amplitude A then becomes

$$A = nN_A\left\{\sum b_{dendr} + \gamma N_{ex}(b_D - b_H) - \left(1 - \frac{(\alpha - 1)\upsilon_{cavity}}{\upsilon_{dendr}}\right)\frac{\upsilon_{dendr}}{\upsilon_{water}}[b_{H_2O} + \gamma(b_{D_2O} - b_{H_2O})]\right\}^2 \tag{6}$$

Equation 6 consists of only two unknown variables, α and υ_{dendr}, while υ_{cavity} is the available water accessible volume inside a dendrimer that can be calculated as $(4\pi/3)R_b^3 - \upsilon_{dendr}$ with the given boundary radius, R_b, estimated from R_{HS} and σ. It is then possible to extract the water density ratio, α, if υ_{dendr} is known a priori from different experimental methods.

III. Results and Discussion

The SANS absolute intensity distributions and the corresponding model fitting curves obtained from G6 PAMAM dendrimer aqueous solutions at four different contrast conditions are presented in Figure 1. The contribution of the incoherent scattering, I_{INC}, has been subtracted from all curves. An expected strong dependence of the scattering amplitude A on the scattering contrast is clearly seen in a satisfactory agreement with the theory. Along with the results of G4 and G5, the fitted parameters R_{HS}, σ, and R_G calculated from eq 3 are shown in Table 1. Within the uncertainty indicated by the statistical error, R_G remains unchanged at different H_2O/D_2O mixture ratio. Our observation is essentially in agreement with the conclusions obtained from the SANS experiment of PAMAM dendrimers with diphenyl ether end groups dissolved in the mixtures of deuterated and protonated dimethylacetamide (DMA) solutions carried out by Ballauff et al.[9,10] It is also consistent with extensive experimental evidence obtained from various micellar systems.[18] However, this independence of R_G presents a stark

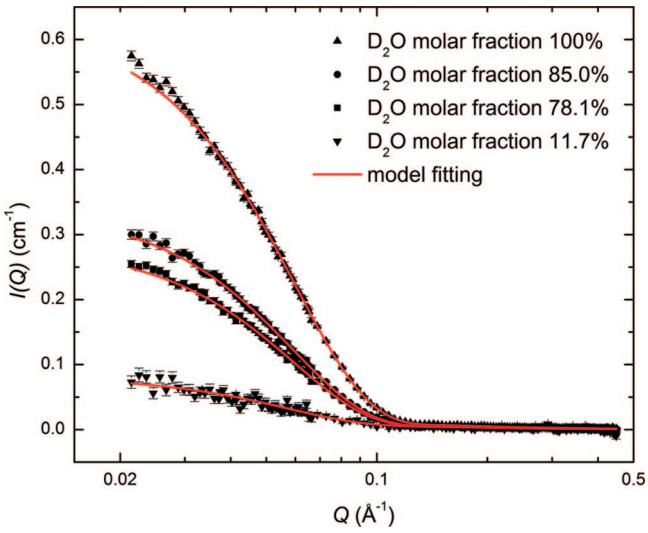

Figure 1. SANS intensity distributions $I(Q)$ of the G6 PAMAM dendrimer aqueous solutions at about 10 mg/mL with different γ values. Solid red lines are the model fitting results. The incoherent background has been subtracted.

Table 1. Structural Parameters of G4 to G6 PAMAM Dendrimer Obtained through Our Model Fitting at Different D_2O/H_2O Mole Ratio

	D_2O (%)	R_{HS} (Å)	σ (Å)	R_G (Å)
G4	1.00	20.3 ± 0.4	8.5 ± 0.5	18.9 ± 0.8
	0.891	22.5 ± 0.4	5.2 ± 0.9	18.6 ± 0.9
	0.78	23.0 ± 0.5	3.7 ± 1.8	18.4 ± 1.2
	0.06	21 ± 5	5 ± 10	18 ± 11
G5	1.00	25.2 ± 0.4	10.4 ± 0.5	23.3 ± 0.7
	0.895	25.9 ± 0.6	10.1 ± 0.8	23.6 ± 1.2
	0.792	27.0 ± 0.6	8.1 ± 1.0	23.1 ± 1.2
	0.047	29.5 ± 1.5	1 ± 22	22.9 ± 3.6
G6	1.00	31.1 ± 0.3	13.4 ± 0.4	29.2 ± 0.6
	0.85	31.1 ± 0.7	13.6 ± 0.8	29.3 ± 1.3
	0.781	32.0 ± 0.7	12.5 ± 0.9	29.1 ± 1.4
	0.117	33 ± 6	13 ± 8	30.2 ± 11.4

contrast to the results reported by Imae et al.:[13] Determined by the Guinier's law, the R_G of G5 PAMAM dendrimers with hydroxyl end groups is found to decrease upon increasing the H_2O molecular fraction in aqueous solvent. We would like to point out the existence of possible dendrimer aggregates in solution with high pH value, which give rise to an intensity upturn at low angle scattering. Although the reasons for the formation of aggregates still remain unclear, their presence in a measured sample certainly affects the accuracy of obtained R_G through the Guinier plot.

Further upon increasing the H_2O molecular ratio in the solvent, the signal-to-noise ratio of the SANS scattering intensity decreases progressively due to the decrease of the scattering length density contrast and the increase of the incoherent background. Consequently, larger statistical errors in the analyzed R_{HS} and σ are observed for the samples with smaller D_2O molecular fraction. Therefore, in order to minimize the uncertainty of the estimated physical quantities, such as the average number of associating water and the volume of the intramolecular cavity, the required structural information is obtained by analyzing the scattering intensity with the highest contrast obtained from the sample of 100% D_2O molecular fraction in the solvent.

Figure 2 gives the square root of the scattering amplitude A normalized to the dendrimer weight fraction as a function of D_2O molar fraction, γ. The expected linear relationship between the square root of A and γ indicates the soundness of our analysis method. The matching point determined from the linear

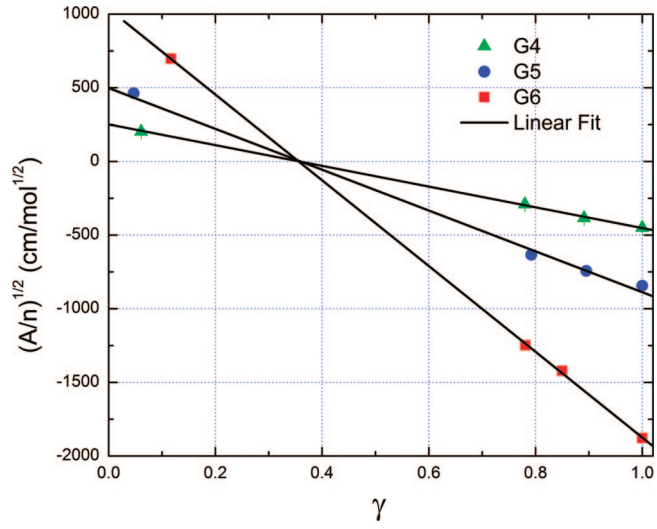

Figure 2. Square root of the scattering amplitude A normalized by the concentration of dendrimers, n, as a function of D_2O molar fraction, γ. The volume of dendrimers is directly determined from the contrast matching points.

Table 2. Volume of a Dendrimer and Fraction of Water Accessible Volume Calculated at Different Boundary Radius[a]

	v_{dendr} (nm^3)	water volume fraction calculated by R_G	water volume fraction calculated by R_{HS}	water volume fraction calculated by $R_{HS} + \sigma$
G4	18.0 ± 0.6	0.36 ± 0.09	0.49 ± 0.04	0.82 ± 0.02
		(0.31 ± 0.09)	(0.45 ± 0.05)	(0.81 ± 0.02)
G5	36.3 ± 0.9	0.31 ± 0.06	0.46 ± 0.03	0.81± 0.01
		(0.26 ± 0.07)	(0.41 ± 0.03)	(0.79 ± 0.01)
G6	73.8 ± 1.8	0.29 ± 0.05	0.41 ± 0.03	0.80 ± 0.01
		(0.24 ± 0.05)	(0.37 ± 0.03)	(0.79 ± 0.01)

[a] Values in parentheses are the results after considering the density change.

fit is found for a D_2O molar fraction of 0.36(1) for all three generations, indicating an independence of the density of PAMAM polymeric constituent components on generations. Quantitatively, this result is considerably different from the matching point of G5 PAMAM dendrimers with hydroxyl end groups, which is reported at H_2O molar fraction of 0. 726 (27.4% of D_2O) by Imae et al.[13] However, in ref 13, the error-bar analysis is not incorporated in the calculation when the physical variables are evaluated. Moreover, the expected linear dependence of square root of the experimental value of the zero angle scattering intensity $[I(0)]^{1/2}$ on H_2O weight fraction is also absent, which could potentially affect the absolute value of the contrast matching point.

Based on our determined matching point and assuming that the water density is identical inside and outside a dendrimer, the molecular volume of a dendrimer v_{dendr} can be directly calculated via eq 4, and the results are given in Table 2. The specific volume of the dendrimer molecule, which is defined as the molecular volume normalized to the molecular weight deduced from the chemical structure, can also be calculated. Based on the values of v_{dendr} given in Table 2, a generational independent value of 0.76(2) mL/g is found.

Alternatively, v_{dendr} can be determined by the slope of the linear fit in Figure 2 as indicated by eq 4. In comparison to the precedent value, smaller specific volume of 0.711(6), 0.694(4), and 0.717(4) mL/g for G4, G5, and G6 are obtained, respectively. These slight quantitative differences could result from the possible uncertainty in the dendrimer concentration of the samples, which could introduce a variation in the scattering amplitude A. Another possible reason might be the small

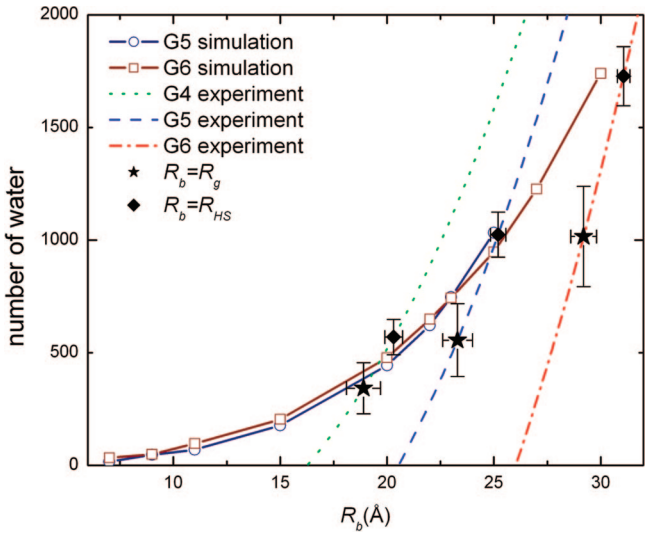

Figure 3. Number of water inside a sphere at the center of dendrimers as a function of the sphere radius. The computer simulation results are transcribed from ref 4 (solid lines). By subtracting the volume of the dendrimer from the sphere with the boundary radius, R_b, the number of water molecules inside a dendrimer is obtained (dashed lines). The star and diamond points give values calculated when $R_b = R_G$ and $R_b = R_{HS}$.

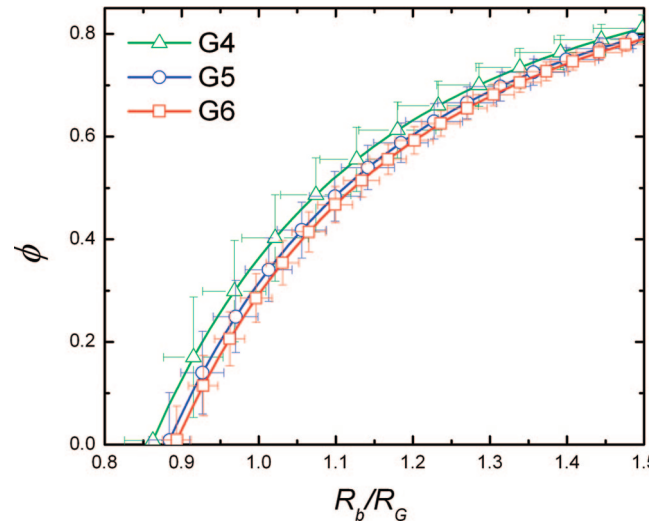

Figure 4. Volume fraction of water accessible region Φ as a function of radius R_b normalized to radii of gyration. Φ is defined as $(v - v_{dendr})/v$, where v is molecular volume of dendrimer, evaluated by either R_b, and v_{dendr} the volume of the polymeric constituent components of a single dendrimer.

influence of the interdendrimer structure factor, $S(Q)$, as pointed out by ref 9. Since $S(Q)$ is only a function of the volume fraction when the interparticle potential remains unchanged, the effect of $S(Q)$ on A can be considered as a simple scalar because our sample concentration is kept constant at ~ 1 wt % during the experiment. It is well-known that the change of A by a constant does not alter the matching point. Therefore, in this study, the molecular volume calculated from the matching point approach is used to estimate the number of associated water molecules.

Assessing the molecular solvent content of PAMAM dendrimer has been the focus of many computational works incorporating the solvent effect explicitly: Wagner et al. calculated the pair correlation function of the solvent with respect to the molecular center and predicted a nonuniform distribution of water molecules throughout the dendrimer interior.[7] Larson et al. calculated the average number of water associated with the branch points of G5 PAMAM dendrimer. The MD work carried out by Goddard et al. showed a steady increase of associated water molecules as a function of the distance from the molecular center[4] and provides a convenient comparison with our experimental result.

From the experimental perspective, the number of penetrating water molecules can be calculated straightforwardly by subtracting the volume occupied by the constitutent components of dendrimer, v_{dendr}, from the overall molecular volume, which is a volume of a sphere with its boundary radius, R_b, normalized to the molecular volume of water, 30 Å^3. However, this calculation is severely compounded by the ill-defined molecular boundary, R_b, due to the swollen corona of the dendrimer periphery. Special care is obviously necessary for a quantitative evaluation of the water penetration inside a dendrimer molecule.

Figure 3 presents the water content of G4−6 PAMAM dendrimers estimated experimentally and predicted by MD simulation.[4] MD simulation has shown that the penetration of water is greatly facilitated by the presence of hydrogen bonds network inside a dendrimer. The internal cavities in the vicinity of the molecular central region are found to be accessible for water molecules. Hence, the number of associated water is seen to increase steadily from the molecular center as a function of the radial distance r_b. However, unlike the MD simulation modeling the spatial distribution of water and polymer at the atomic level, these microscopic details are averaged over in our model, and therefore it is not possible to access a detailed spatial distribution of confined water experimentally. However, the total number of water molecules inside the dendrimer can be estimated as shown in Figure 3 with different boundary radius, R_b. The lower limit of the experimental curves represents a dendrimer conformation where all the segments are collapsed to form a uniform sphere without any internal water molecules. The corresponding radius is calculated using the radius of the hard sphere R_L to define the dendrimer volume v_{dendr}, namely $v_{dendr} = 4/3\pi R_L^3$ (R_L ~ 16 Å for G4, 21 Å for G5, and 26 Å for G6). The number of water molecules increases as the boundary radius, R_b, increases.

Computationally, it has been demonstrated that, along the radial direction from the molecular center, the intramolecular polymer density profile is seen to remain at a constant level within the distance of R_G and decay monotonically beyond that. Hence, if we assume R_G as the boundary radius, the estimated water molecule number inside a dendrimer is about 335 ± 120, 556 ± 162, and 1016 ± 223 for G4, G5, and G6, respectively. Given the volume of one water molecule to be 30 Å^3, the internal volume of the cavity occupied by water, denoted as v_{RG}, is then calculated as 10 ± 4, 17 ± 5, and 30 ± 7 nm^3 for G4, G5, and G6, respectively. The corresponding fraction of accessible volume is around 30% as shown in Table 2. According to the fuzzy-ball model, $P(Q)$, the molecular boundary value can be chosen as R_{HS}. The calculated water number for G4, G5, and G6 is 570 ± 78, 1024 ± 100, and 1728 ± 131 and shown as solid diamonds in Figure 3, which agrees very well with the computer simulation results. This might indicate that the appropriate boundary radius to delimit inside and outside water molecules is R_{HS}.

Once v_{dendr} is known, the volume fraction of cavity inside a dendrimer can be estimated. Figure 4 shows the accessible water volume fraction as a function of R_b normalized by the corresponding R_G. Surprisingly, we find that within the statistical error the lines corresponding to different dendrimer generations collapse into one single curve even though a slight increase of the water volume fraction with decreasing dendrimer generation might be discerned. This observation indicates that, as long as the density profile of a dendrimer does not significantly change with the generation numbers, the accessible water volume fraction of a single dendrimer is almost independent from

dendrimer generation. However, it has been speculated that due to the steric excluded-volume interaction among the constituent components of the dendrimer branches, dendrimer of higher generations possess less available intramolecular space.[1] In this report only G4−6 PAMAM dendrimers have been studied, and SANS investigation of other generations of dendrimers is currently ongoing to test this hypothesis of spatial constraints. Since the real molecular boundary, R_b, is expected to be located between R_G and $R_{HS} + \sigma$, the volume fraction ranges from ~30% to ~80%. When R_b is assumed to be R_{HS}, the corresponding volume fraction of accessible water volume is about 45%; namely, about half-space inside a dendrimer is accessible by other molecules.

Furthermore, we would like to point out that the PAMAM dendrimer specific volume of 0.76 mL/g obtained from our SANS experiment is smaller than the result of 0.82 mL/g obtained from density measurement of G4 and G5 PAMAM dendrimers in a nonsolvent condition by Dendritech Inc.[14,19] The reason for the difference could be due to the fact that either the specific volume of PAMAM changes for different solvent condition or the density of water inside the PAMAM changes while the volume of the PAMAM polymer chain remains the same. In the latter case, the average density of the water inside a dendrimer is expected to change by a factor of α according to the calculations based on eqs 4 and 6. If we assume that the specific volume of dendrimer in water remains 0.82 mL/g, α is found to be 1.2 ± 0.1, 1.10 ± 0.06, or 1.019 ± 0.008 when R_G, R_{HS}, or $R_{HS} + \sigma$ is used to estimate the dendrimer molecular volume, respectively. Either way, the average water density inside the dendrimers is considerably higher than bulk water. Although generally water is incompressible around room temperature, it has been shown that the density of water confined in nanopores or on surface can be significantly different from its bulk density. For example, a number of computer simulation results indicate that the average water density around the vicinity of charged DNA and protein surfaces is significantly larger than the bulk density.[20,21] Recent experiments show that the confined water in MCM-41 is 8% denser than the bulk water at room temperature,[22] and the hydration water density on protein surface is ≈10% larger than its bulk value.[23] These reported values are close to the density of water observed in the current report if R_b is set to be R_{HS}. With the increase of average internal water density, the corresponding number of water molecules inside a dendrimer is seen to remain unchanged. Consequently, the water accessible internal volume will be slightly affected by the water density change as shown in Table 2. Finally, it is instructive to indicate that the conclusion still holds that the fraction of available volume of a dendrimer is almost generation independent from G4 to G6.

IV. Conclusions

Contrast variation SANS experiment has been carried out to investigate the intramolecular water content of G4−6 PAMAM dendrimers in aqueous solution. On the basis of our model fitting, significant amount of water has been found inside a dendrimer, which is quantitatively consistent with results of MD simulations. When R_{HS} is chosen as the boundary radius, the estimated number of water molecules is found to agree with the simulation results very well. In addition, the water accessible volume fraction of a dendrimer is found to be independent of the dendrimer generation from G4 to G6. Moreover, assuming that the volume of PAMAM polymer chain remains the same under different solvent conditions, we found that the average density of water inside a dendrimer is higher than the one of bulk water by a factor between 1.2 ± 0.1 and 1.019 ± 0.008. Assuming R_{HS} as the boundary radius, the water density changes by a factor of 1.10 ± 0.06 compared with the bulk water density.

Acknowledgment. We gratefully acknowledge the support from the Laboratory Directed Research and Development Program (Project ID 05125) of ORNL and the partial financial support by U.S. Department of Energy within the Hydrogen Sorption Center of Excellence. The support of the National Institute of Standards and Technology, U.S. Department of Commerce, in providing the neutron research facilities supported under NSF Agreement DMR-0454672 is also acknowledged. Part of this research was done at Oak Ridge National Laboratory's Center for Nanophase Materials Sciences which was sponsored by the Scientific User Facilities Division, Office of Basic Energy Sciences, U.S. Department of Energy.

References and Notes

(1) *Dendrimers (Topics in Current Chemistry)*; Vögtle, F., Ed.; Springer: New York, 1998.
(2) *Dendrimers in Medicine and Biotechnology: New Molecular Tools*; Boas, U., Christensen, J. B., Heegaard, P. M., Eds.; Royal Society of Chemistry: London, 2006.
(3) Ballauff, M.; Likos, C. N. *Angew. Chem., Int. Ed.* **2004**, *43*, 2998–3020.
(4) Maiti, P. K.; Çain, T.; Lin, S.-T.; Goddard, W. A. *Macromolecules* **2005**, *38*, 979–991.
(5) Lin, S.-T.; Maiti, P. K.; Goddard, W. A. *J. Phys. Chem. B* **2005**, *109*, 8663–8672.
(6) Maiti, P. K.; Goddard, W. A. *J. Phys. Chem. B* **2006**, *110*, 25628–25632.
(7) Opitz, A. W.; Wagner, N. J. *J. Polym. Sci., Part B: Polym. Phys.* **2006**, *44*, 3062–3077.
(8) Lee, H.; Baker, J. R.; Larson, R. G. *J. Phys. Chem. B* **2006**, *110*, 4014–4019.
(9) Pötschke, D.; Ballauff, M.; Lindner, P.; Fischer, M.; Vögtle, F. *Macromolecules* **1999**, *32*, 4079–4087.
(10) Rosenfeldt, S.; Dingenouts, N.; Ballauff, M.; Werner, N.; Vögtle, F.; Lindner, P. *Macromolecules* **2002**, *35*, 8098–8105.
(11) Topp, A.; Bauer, B. J.; Kilmash, K. W.; Spindler, R.; Tomalia, D. A.; Amis, E. J. *Macromolecules* **1999**, *32*, 7226–7231.
(12) Huang, Q. R.; Dubin, P. L.; Lal, J.; Moorefield, C. N.; Newkome, G. R. *Langmuir* **2005**, *21*, 2737–2742.
(13) Imae, T.; Funayama, K.; Aoi, K.; Tsutsumiuchi, K.; Okada, M.; Furusaka, M. *Langmuir* **1999**, *15*, 4076–4084.
(14) In their own activities as scientific institutions, NIST and ORNL use many different materials, products, types of equipment, and services. However, NIST and ORNL do not approve, recommend, or endorse any product or proprietary material.
(15) Chen, W.-R.; Porcar, L.; Liu, Y.; Butler, P. D.; Magid, L. J. *Macromolecules* **2007**, *40*, 5887–5898.
(16) Kline, S. R. *J. Appl. Crystallogr.* **2006**, *39*, 895–900.
(17) Lawrence, S. A. *Amines: Synthesis, Properties and Applications*, 1st ed.; Cambridge University Press: Cambridge, 2006.
(18) Chen, S.-H. *Annu. Rev. Phys. Chem.* **1986**, *37*, 351–399.
(19) The information is available at www.dendritech.com.
(20) Merzel, F.; Smith, J. C. *Proc. Natl. Acad. Sci. U.S.A.* **2002**, *99*, 5378.
(21) Feig, M.; Pettitt, B. M. *Biopolymers* **1998**, *48*, 199.
(22) Liu, D.; Zhang, Y.; Liu, Y.; Wu, J.; Chen, C. C.; Mou, C. Y.; Chen, S. H. *J. Phys. Chem. B* **2008**, *112*, 4309.
(23) Svergun, D. I.; Richard, S.; Koch, M. H. J.; Sayers, Z.; Kuprin, S.; Zaccai, G. *Proc. Natl. Acad. Sci. U.S.A.* **1998**, *95*, 2267.

MA801555J